

Electrical Characteristics of IGZO Thin Film Transistors Fabricated by Magnetron Sputtering with Controlled Mean Free Path of Sputtered Particles

Kai Chen^{1,2}, Rui Zhang¹, Junkang Li^{1*}, Yunlong Li^{1,2,3*}

¹College of Integrated Circuits, Zhejiang University, Hangzhou 311200, China

²Zhejiang ICsprout Semiconductor Co., Ltd, Hangzhou 311200, China

³State Key Laboratory of Silicon and Advanced Semiconductor Materials, Zhejiang University, Hangzhou 310027, China

*Corresponding Author's Email: lijunkang@zju.edu.cn; bta@zju.edu.cn

ABSTRACT

This study investigates the optimization of indium gallium zinc oxide (IGZO) thin film transistors (TFT) by refining magnetron sputtering parameters and applying post-deposition annealing. Controlling argon-to-oxygen ratios and gas flow influenced the mean free path, enhancing film density and electronic properties. X-ray photoelectron spectroscopy (XPS) confirmed that while higher oxygen ratios during deposition improved metal-oxygen bonding, post-deposition annealing was critical in minimizing defects and enhancing film stability. The optimized IGZO TFTs demonstrated a stable threshold voltage, a subthreshold swing of 100 mV/dec, and a hysteresis of 42 mV, advancing low-power oxide TFT technology.

Keywords—IGZO; TFT; Sputtering conditions; Mean free path; Annealing

INTRODUCTION

Indium gallium zinc oxide (IGZO) thin films show strong potential as TFT channel materials due to their high electron mobility, low off-current, and adaptability for flexible electronics [1, 2]. These properties are desirable in applications such as displays, wearables, and low-power devices [3-5]. Achieving high-quality IGZO films is critical for optimizing device performance, with popular fabrication methods including atomic layer deposition (ALD) and magnetron sputtering [6]. While ALD ensures uniform film coverage [7], magnetron sputtering provides a faster deposition rate with precise control over film thickness and composition, making it favorable for scalable manufacturing, though it is sensitive to a range of process parameters

Magnetron sputtering offers flexibility in adjusting deposition parameters, such as the choice of gases (e.g., argon, oxygen), gas flow rates, chamber pressure, and sputtering power [8]. However, challenges like substrate temperature control and precise low oxygen flow regulation can complicate the process. Understanding the impact of these factors on IGZO film properties is crucial for achieving high-performance devices.

This research systematically explores how variations in gas flow ratios, chamber pressure, and sputtering time affect IGZO films and TFT performance. Adjusting the argon-to-oxygen ratio affects the mean free path of sputtered particles, which in turn shapes film characteristics. XPS analysis reveals that higher oxygen content enhances metal-oxygen bond formation and reduces oxygen vacancies, while post-deposition oxygen annealing further minimizes defects, improving device performance. Optimized conditions, particularly for thinner IGZO films, yield enhanced on-current, a subthreshold swing as low as 100 mV/dec, and mobility reaching 11.6 cm²/V·s. These results offer practical insights for fine-tuning sputtering conditions, supporting the development of high-performance, low-power oxide TFTs.

DEVICE FABRICATION

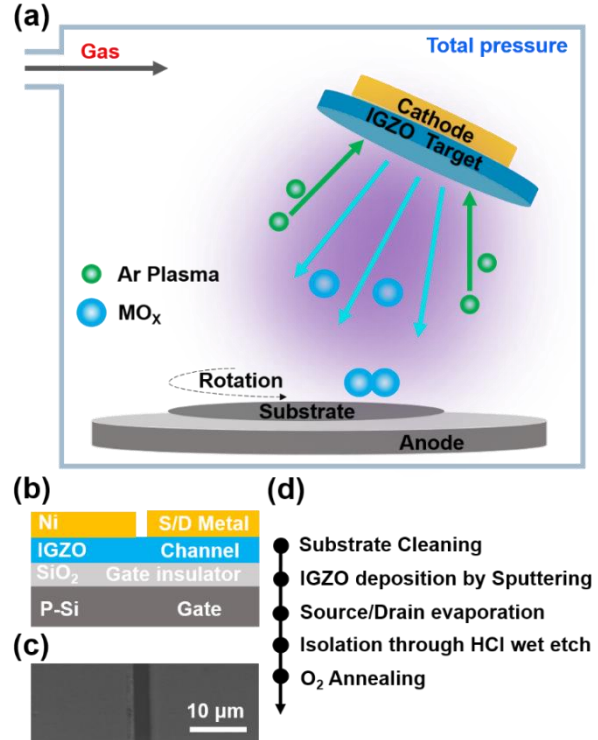


Fig. 1. (a) Schematic illustration of the IGZO deposition by magnetron sputtering process (b) Structure of the fabricated bottom-gated IGZO TFT (c) Top view SEM image of IGZO TFT with 3 μm channel length (d) Key process steps

The IGZO magnetron sputtering process, shown in **Fig. 1(a)**, uses a 3-inch IGZO target (In:Ga:Zn atomic ratio of 2:2:1) backed by a 3 mm copper plate, positioned 140 mm from the anode. RF power of 100 W is applied, with the substrate rotating at 50% speed at room temperature. Argon and oxygen flow rates control chamber pressure, and sputtering time is adjusted for the desired film thickness. **Fig. 1(b)** shows the bottom-gate structure of the IGZO TFTs, and **Fig. 1(c)** presents a top-view SEM image with a 3 μm channel length. **Fig. 1(d)** illustrates the fabrication process. After IGZO deposition, a 50 nm nickel layer is thermally evaporated for source and drain electrodes, followed by a lift-off process for patterning. The IGZO channel is etched with a 3% diluted HCl solution. Finally, the devices are annealed at 400°C in an oxygen atmosphere.

RESULTS AND DISCUSSION.

A. Influence of Reactive Sputtering Atmosphere Ratios on IGZO Channel Properties in FETs

The XPS spectra in **Fig. 2(a-c)** show the composition of IGZO films deposited at argon-to-oxygen flow ratios of 40:6, 40:8, and 40:10 sccm, corresponding to chamber pressures of 4.5, 4.6, and 4.7 mtorr, respectively. These pressure changes significantly impact film quality, as discussed in subsequent

sections. XPS analysis reveals that higher oxygen flow increases metal-oxygen bonding and reduces oxygen vacancies, improving film stoichiometry, as summarized in **Fig. 2(d)**. **Fig. 2(e)** shows that annealing a 40:6 sccm IGZO film in oxygen for 10 minutes further enhances metal-oxygen bonds and reduces vacancies, improving film quality. This suggests that post-deposition annealing is more effective in reducing vacancies than solely increasing oxygen flow during sputtering. **Fig. 2(f)** compares the transfer characteristics of IGZO TFTs under different conditions. Films without annealing exhibit poor switching behavior. In contrast, annealed film shows clear switching characteristics. These findings suggest that oxygen annealing is more effective than adjusting gas flow when very low oxygen flows cannot be achieved [9].

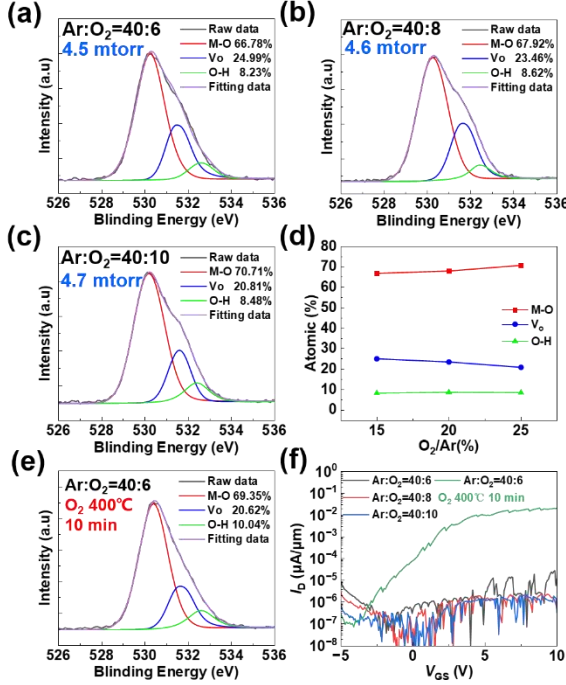


Fig. 2. (a-c) XPS spectra of IGZO films at different argon-to-oxygen gas flow ratios (d) Atomic percentages of M-O, Vo and O-H at different argon-to-oxygen gas flow ratios (e) XPS spectra of IGZO film at 40:6 argon-to-oxygen gas flow ratio after annealing (f) Transfer curves of the above IGZO TFTs

The effects of argon-only deposition on IGZO films were also studied. **Fig. 3(a)** and **Fig. 3(b)** show XPS spectra for films deposited at argon flow rates of 20 sccm and 30 sccm, with pressures of 3.1 mtorr and 3.7 mtorr, respectively. Increased argon flow enhanced metal-oxygen bonding and reduced oxygen vacancies. Post-annealing XPS spectra (**Fig. 3(c)** and **Fig. 3(d)**) show further increases in metal-oxygen bonds and reduced vacancies after 10 minutes of annealing at 400°C in an oxygen atmosphere. Transfer characteristics in **Fig. 3(e)** and **Fig. 3(f)** reveal that, prior to annealing, lower argon flow results in a 2V turn-on voltage, while higher flow shifts it to -2.5V. After annealing, the curves shift positively, indicating improved oxygen incorporation [10].

Based on the data in **Table I**, the argon-to-oxygen flow ratios, chamber pressures, mean free path (MFP) [11], and average collision numbers for the IGZO deposition process are summarized. As chamber pressure increases, the MFP decreases, indicating more frequent particle collisions. For instance, at an Ar:O₂ ratio of 40:10, the highest pressure (0.626 Pa) results in an MFP of 11.6 mm and an average collision count of 12.1 over the 140 mm distance from target to substrate.

In contrast, at a 20:0 ratio, the pressure drops to 0.346 Pa, extending the MFP to 21 mm and reducing the collision count to 6.6.

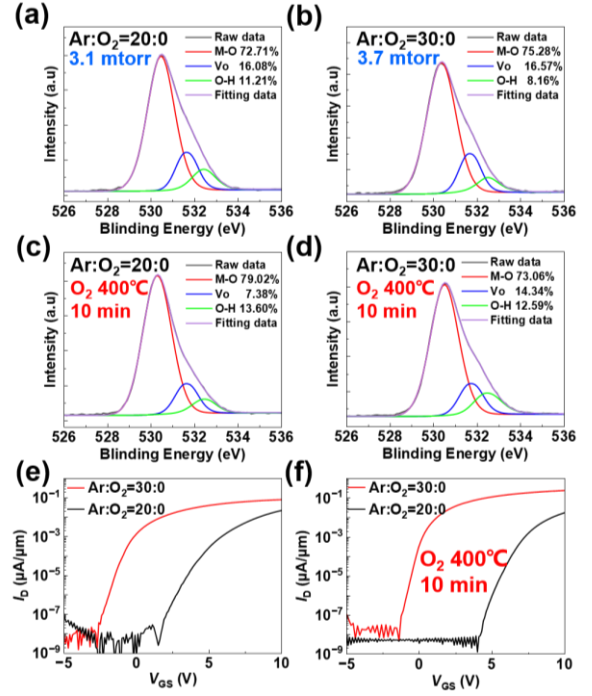


Fig. 3. (a, b) XPS spectra of IGZO films at different argon gas flow rates. (c, d) XPS spectra of IGZO films after oxygen annealing. (e) Transfer curves of as-deposited IGZO TFTs. (f) Transfer curves of IGZO TFTs after oxygen annealing.

TABLE I

Mean free path and average collision frequency of molecules in the chamber under different argon and oxygen flow rates

Ar : O ₂ ratio	Total pressure (Pa)	MFP (mm)	N(D,P)
40 : 10	0.626	11.6	12.1
40 : 8	0.613	11.9	11.7
40 : 6	0.599	12.4	11.2
30 : 0	0.490	14.8	9.4
20 : 0	0.346	21.0	6.6

The mean free path λ can be calculated using the following formula [11]:

$$\lambda = \frac{k_B \cdot T}{\sqrt{2} \cdot \pi \cdot d^2 \cdot P}$$

Where k_B is the Boltzmann constant, T is the absolute temperature in Kelvin, d is the effective diameter of the gas molecule, P is the chamber pressure.

Once the MFP is calculated, the average collision number N from the target to the substrate (distance $L=140$ mm) can be estimated by:

$$N = \frac{L}{\lambda}$$

A shorter MFP and higher collision frequency result in more energy loss for sputtered particles due to interactions with the vapor phase, reducing their mobility upon reaching the substrate surface. This can affect the film's density and structural relaxation, as excessive vapor-phase reactions or high pressures may yield low-density films with weakly bonded oxygen, ultimately lowering film quality. Thus, optimizing chamber pressure and MFP is essential for producing high-quality, stable a-IGZO films with desired properties.

B. Influence of sputtering time (thickness) on IGZO TFT performance

Building on previous sputtering optimizations, the effect of IGZO thickness on TFT characteristics was examined. As shown in **Fig. 4(a)** and **4(b)**, reducing IGZO thickness from 76 nm to 27 nm and 15 nm results in a positive shift in turn-on voltage: the 76 nm device remains conductive without a clear turn-on point, while the 27 nm device turns on around -5V, and the 15 nm device shows a turn-on voltage near 0V with well-defined switching behavior. AFM analysis (**Fig. 4(c)** and **4(d)**) indicates that the 15 nm film has low surface roughness ($R_q=0.341$ nm, $R_a=0.267$ nm), supporting stable electrical performance. These findings suggest that reduced thickness improves on-off characteristics and allows for more precise turn-on voltage control [12].

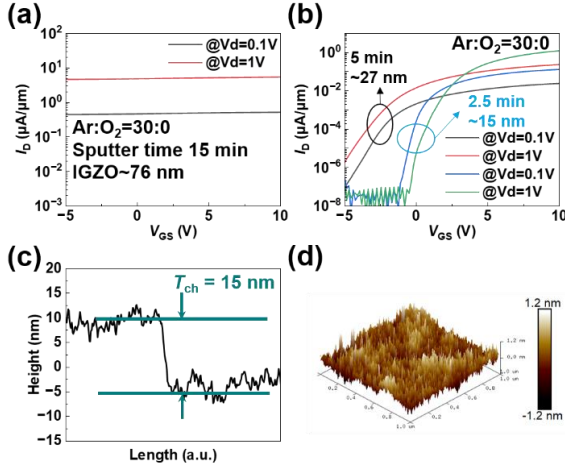


Fig. 4. (a) Transfer characteristic curve of an IGZO TFT with 76 nm thickness (sputtering time: 15 min). (b) Transfer characteristic curve of IGZO TFTs with 27 nm (5 min) and 15 nm (2.5 min) thickness. (c) AFM image of IGZO with a thickness of 15 nm. (d) Surface roughness image of the IGZO transistor channel area.

C. High-performance IGZO thin-film transistor obtained by optimizing sputtering conditions

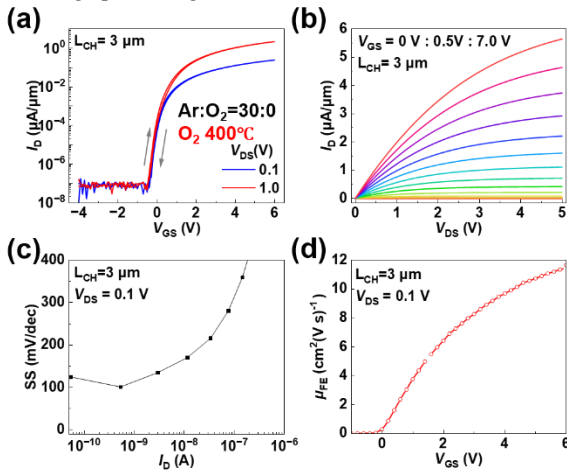


Fig. 5. (a) Transfer characteristic curve of a 15 nm IGZO channel at 30 sccm argon flow rate after 30 minutes of oxygen annealing. (b) Corresponding transport characteristic curve. (c) Subthreshold swing versus drain current density. (d) Linear mobility.

Further improvements in IGZO TFT performance were achieved through post-deposition annealing. **Fig. 5(a)** illustrates the transfer characteristics of a 15 nm IGZO TFT annealed at 400°C in an oxygen atmosphere for 30 minutes, showing well-defined on/off switching and a low hysteresis of 42 mV, demonstrating reduced defect states and stable channel

properties. **Fig. 5(b)** confirms high contact quality, with a maximum on-current density of 5 $\mu\text{A}/\mu\text{m}$. The device achieved a low subthreshold swing (SS) of 100 mV/dec (**Fig. 5(c)**), reflecting efficient channel control and minimized leakage. Finally, linear mobility reached 11.6 $\text{cm}^2/\text{V}\cdot\text{s}$ (**Fig. 5(d)**), indicating improved carrier transport.

CONCLUSION

This study optimized IGZO TFTs through controlled magnetron sputtering and post-deposition annealing. By adjusting the argon-to-oxygen flow ratio, we controlled film density and electronic properties. XPS analysis revealed that increasing oxygen content during deposition alone did not effectively reduce oxygen vacancies; however, post-deposition annealing in an oxygen atmosphere significantly enhanced metal-oxygen bonding, reduced defects, and stabilized film properties. Under optimal sputtering and annealing conditions, the IGZO TFTs exhibited high performance, including stable threshold voltage, low SS (100 mV/dec), and mobility up to 11.6 $\text{cm}^2/\text{V}\cdot\text{s}$, marking significant progress for low-power, high-performance oxide TFTs.

ACKNOWLEDGEMENTS

This work is supported by National Key R&D Program of China (2022YFF0605803), Zhejiang Key R&D project (2022C01063, 2023C01017).

REFERENCES

- [1] K. Nomura, H. Ohta, A. Takagi, T. Kamiya, M. Hirano, and H. Hosono, "Room-temperature fabrication of transparent flexible thin-film transistors using amorphous oxide semiconductors," *nature*, vol. 432, no. 7016, pp. 488-492, 2004.
- [2] S. Lee and A. Nathan, "Subthreshold Schottky-barrier thin-film transistors with ultralow power and high intrinsic gain," *Science*, vol. 354, no. 6310, pp. 302-304, 2016.
- [3] E. Fortunato, P. Barquinha, and R. Martins, "Oxide semiconductor thin-film transistors: a review of recent advances," *Advanced materials*, vol. 24, no. 22, pp. 2945-2986, 2012.
- [4] D. Geng et al., "Thin-film transistors for large-area electronics," *Nature Electronics*, vol. 6, no. 12, pp. 963-972, 2023.
- [5] A. Yan et al., "Thin-Film Transistors for Integrated Circuits: Fundamentals and Recent Progress," *Advanced Functional Materials*, vol. 34, no. 3, p. 2304409, 2024.
- [6] M. H. Cho et al., "Comparative study on performance of IGZO transistors with sputtered and atomic layer deposited channel layer," *IEEE Transactions on Electron Devices*, vol. 66, no. 4, pp. 1783-1788, 2019.
- [7] S. M. George, "Atomic layer deposition: an overview," *Chemical reviews*, vol. 110, no. 1, pp. 111-131, 2010.
- [8] P. J. Kelly and R. D. Arnell, "Magnetron sputtering: a review of recent developments and applications," *Vacuum*, vol. 56, no. 3, pp. 159-172, 2000.
- [9] T. Mudgal, N. Walsh, R. G. Manley, and K. D. Hirschman, "Impact of annealing on contact formation and stability of IGZO TFTs," *ECS Transactions*, vol. 61, no. 4, p. 405, 2014.
- [10] C.-S. Fuh, S. M. Sze, P.-T. Liu, L.-F. Teng, and Y.-T. Chou, "Role of environmental and annealing conditions on the passivation-free in-Ga-Zn-O TFT," *Thin solid films*, vol. 520, no. 5, pp. 1489-1494, 2011.
- [11] W. Zhang et al., "Influence of the electron mean free path on the resistivity of thin metal films," *Microelectronic engineering*, vol. 76, no. 1-4, pp. 146-152, 2004.
- [12] Y. Li et al., "Effect of channel thickness on electrical performance of amorphous IGZO thin-film transistor with atomic layer deposited alumina oxide dielectric," *Current Applied Physics*, vol. 14, no. 7, pp. 941-945, 2014.